Proposal for CLAS approved analysis

Evaluation of the moments of the structure function F_2 at intermediate Q^2

M. Osipenko[a], G. Ricco[b,c], M. Taiuti[b],
M. Anghinolfi[c], M. Battaglieri[c], R. De Vita[c],
E. Golovach[d], G. Fedotov[a], B. Ishkhanov[a,d],
V. Mokeev[d], M. Ripani[c], V. Sapunenko[c,d]
S. Simula[e]

[a] *Physics Department of Moscow State University,*
[b] *Dipartimento di Fisica, Università di Genova,*
[c] *INFN, sez. di Genova*
[d] *Nuclear Physics Institute of Moscow State University*
[e] *INFN, sez. di Roma III*

Abstract

We propose to study inclusive inelastic scattering on hydrogen and nuclei using CLAS and world electroproduction data. The proposed analysis will only consider data runs with beam time already approved.

The main goal of these studies will be a direct evaluation of the moments of the structure function F_2, which implies numerical integration of the experimental data over x at fixed Q^2, in the entire Q^2 range available. This experimental information will allow us to extract the contribution of the higher twists related to multiparton correlation effects. Moreover the comparison with theoretical predictions either based on first-principle calculations, like lattice QCD simulations, or obtained from models of the nucleon structure may represent an important test of the nonperturbative QCD regime.

Contents

Chapter 1

Physics Motivations

1.1 Introduction

The analysis of inelastic electron scattering experiments in the GeV energy region shows some interesting features:

1. At high W (> 3 GeV), proton and deuteron data exhibit *precocious scaling* around a photon mass scale of 1-2 GeV; the experimental cross section approaches the perturbative behavior, as determined by the nucleon structure functions, with the remaining discrepancy still compatible with "power corrections", as predicted in the QCD framework [1]. At lower W the resonances and underlying continuous cross section show a very similar Q^2 evolution (*local duality*) [2]. This effect, up to now poorly understood, seems to be quite general [3] and casts some doubt on the consistency of commonly followed separation procedures between the two components in data analysis or phenomenological models.

2. Data on nuclei show the influence of nuclear matter on nucleon excitation both at high W (EMC effect) and in the resonance region, where P_{33} and D_{13} transition form factors have been reported to decrease with increasing Q^2 faster than in free nucleons [4].

These physics issues, presented in more detail in the following two chapters, suggest a systematic analysis of inclusive inelastic cross sections in proton, deuteron and nuclei, using CLAS data at all available energies could yield important information. In chapter three, the reliability of inclusive CLAS data from preliminary analysis and the covered kinematic range will be discussed.

1.2 The Proton and The Deuteron

The Operator Product Expansion (OPE) of the virtual photon-nucleon scattering amplitude leads to a description of the complete Q^2 evolution for the moments of the nucleon structure functions:

$$M_n^{CN}(Q^2) = \int_0^\infty dx x^{(n-2)} F_2(x,Q^2) = \sum_{\tau=2k}^{\infty} E_{n\tau}(\mu,Q^2) O_{n\tau}(\mu) \left(\frac{\mu^2}{Q^2}\right)^{\frac{1}{2}(\tau-2)} \tag{1.1}$$

where $k = 1, 2, ...,$ $M_n^{CN}(Q^2)$ is the n-th Cornwell-Norton moment of the (asymptotic) structure function for a "massless" nucleon $F_2(x,Q^2)$; μ is the renormalization scale (about 1 GeV), $O_{n\tau}(\mu)$ is the reduced matrix element of operators with definite spin n and twist τ (dimension-spin), related to the nonperturbative structure of the target; $E_{n\tau}(\mu,Q^2)$ is a dimensionless coefficient function describing small distance behavior, which can be perturbatively expressed as a power expansion of the running coupling constant $\alpha_s(Q^2)$.

At Q^2 values comparable with the proton mass (M_p) the structure function still contains non negligible mass dependent terms that produce in Eq. 1.1 further $\frac{M_p^2}{Q^2}$ power corrections (kinematic twists). To avoid these terms, the $M_n^{CN}(Q^2)$ of the "massless" F_2 have to be replaced in 1.1 by the corresponding Nachtmann [5] moments $M_n^N(Q^2)$ of the measured structure function $F_2^{exp}(x,Q^2)$ since:

$$M_n^{CN}(F_2(x,Q^2)) = M_n^N(F_2^{exp}(x,Q^2)) \tag{1.2}$$

For leading twist ($\tau = 2$) one ends up in Leading Order (LO) or Next-to-Leading Order (NLO) with the well known perturbative logarithmic Q^2 evolution of singlet and non singlet F_2 moments. If, however, one wants to estimate possible higher order terms in the α_s perturbative expansion, which completely defines the coefficient function E_n, convergence is affected by the so called renormalon ambiguity which has the general form of power suppressed corrections [5].

For higher twist, $\tau > 2$, power terms $O_{n\tau}(\mu)$ are related to quark-quark and quark-gluon correlations, as illustrated by Fig. 1.1, and should become important at large x and small Q^2.

For an analysis of data on the transverse structure function F_2 Eq. 1.1 can be written [6] in the simplified form (limited to twist 4 and 6):

$$M_n^T(Q^2) = \mu_n^T(Q^2) + \mu_n^{T(IR)}(Q^2) + a_n^{(4)} \left[\frac{\alpha_s(Q^2)}{\alpha_s(\mu^2)}\right]^{\gamma_n^{(4)}} \frac{\mu^2}{Q^2} + a_n^{(6)} \left[\frac{\alpha_s(Q^2)}{\alpha_s(\mu^2)}\right]^{\gamma_n^{(6)}} \frac{\mu^4}{Q^4} \tag{1.3}$$

where $\mu_n^T(Q^2)$ is the leading twist evaluated at NLO in the running coupling constant, $\mu_n^{T(IR)}(Q^2)$ is the renormalon ambiguity, aimed at describing high-order radiative effects beyond the NLO approximation, and the parameters $a_n^{(4)}$, $\gamma_n^{(4)}$, $a_n^{(6)}$, $\gamma_n^{(6)}$ should be related to multiparton correlation effects.

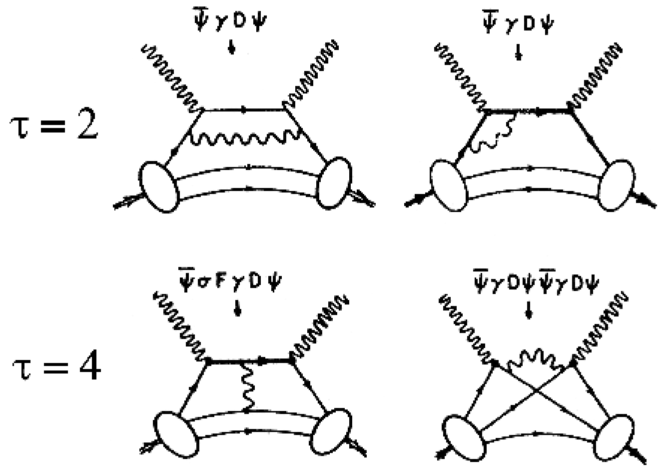

Figure 1.1: Twist diagrams.

A systematic analysis of the Q^2 dependence of the experimental Nachtmann moments $M_n^N(F(x,Q^2))$ in the intermediate Q^2 range ($0.5 < Q^2 < 10$ GeV^2) should therefore allow separation of twist two and higher twist terms in the structure function of nucleons and nuclei. Some preliminary work in this direction has been performed [7] using existing inclusive (SLAC) proton and deuteron data. Nachtmann moments $M_n^N(F(x,Q^2))$ of measured longitudinal $F_L(x,Q^2)$ and transverse $F_2(x,Q^2)$ structure functions have been evaluated for $n = 2,4,6,8$ and in the $1 < Q^2 < 20$ GeV^2 range using current fits of structure functions in the DIS and resonance regions. The obtained moments have been fitted in the whole Q^2 range by the expression 1.3 to extract the contribution of renormalons and higher dynamic twists. All terms due to the infrared renormalon (IR) are governed, for any structure function, by the values of only two parameters: A_2^{IR} and A_4^{IR}, which appear simultaneously for any n, in longitudinal and transverse terms. Higher twist terms are instead identified, for each moment n in Eq. 1.3, by two parameters: $a_n^{(k)}$ coefficient and the effective anomalous dimension $\gamma_n^{(k)}$ (where $k = 4,6$).

The preliminary analysis leads to a few conclusions:

1. The Q^2 dependence of longitudinal moments up to $n = 8$ is fully compatible with renormalon theory using $A_2^{IR} = -0.152$ GeV^2 and $A_4^{IR} = 0.009$ GeV^2, in agreement inside errors with the value extracted from F_3 by the CCFR collaboration [8] and not far from existing theoretical estimations. Present data on longitudinal structure function $F_L(x,Q^2)$ appear therefore consistent with NLO twist 2 calculations plus renormalon ambiguity (Fig. 1.2).

2. If the same A_2^{IR} and A_4^{IR} parameters are now used to evaluate the renormalon contribution to transverse moments of the $F_2(x, Q^2)$ structure function, experimental data for higher moments ($n = 4, 6, 8$) are now definitely underestimated by the sum of NLO twist two plus renormalon and a relevant contribution of dynamic twists has to be included in these moments for the $0.5 < Q^2 < 10$ GeV^2 region (Fig. 1.3).

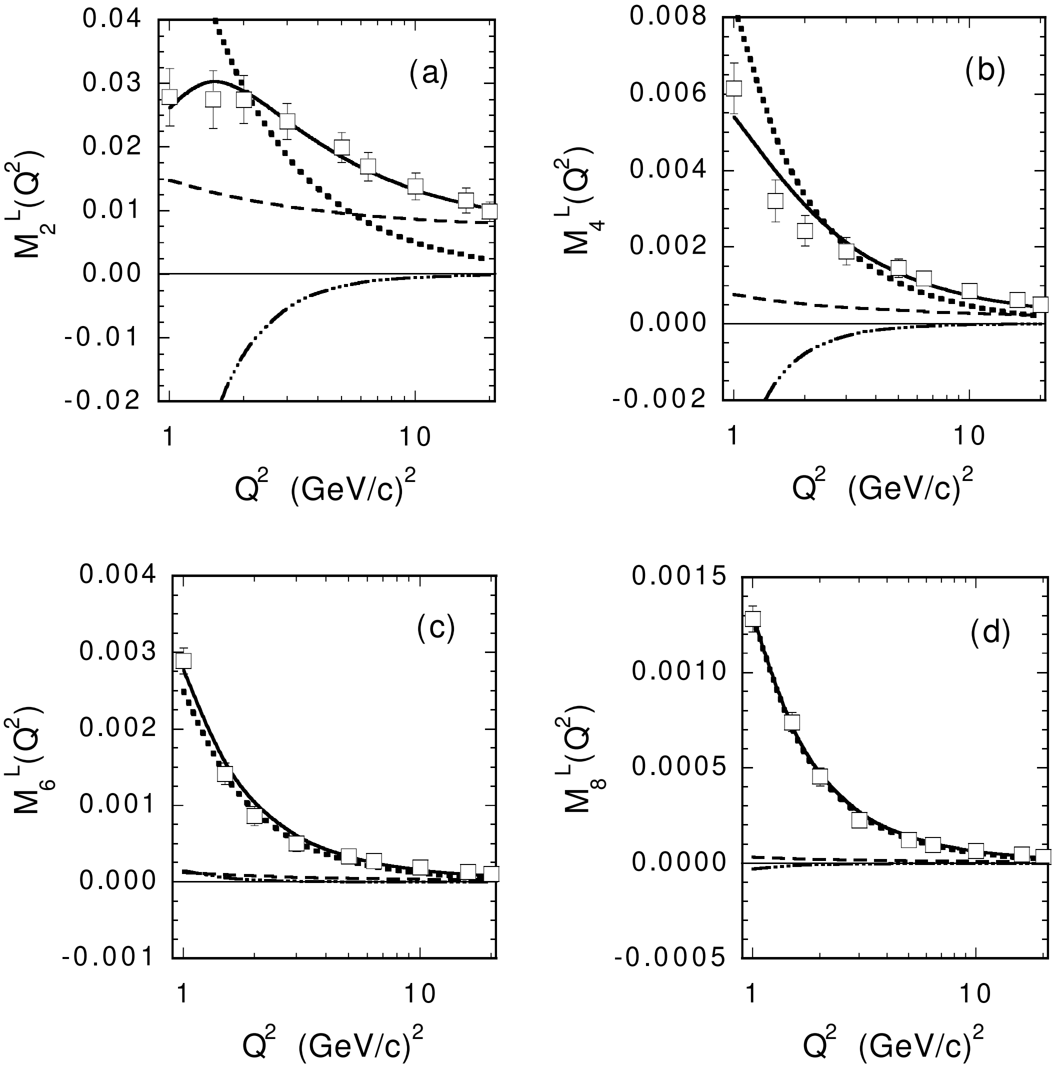

Figure 1.2: Twist analysis of the proton longitudinal moments $M_n^L(Q^2)$ for $n = 2, 4, 6$ and 8, adopting the IR-renormalon model. The open squares represent the pseudo-data; the solid lines are the results fitted by the least-χ^2 procedure to the pseudo-data; the dashed lines are the twist-2 contribution adopting the GRV set of parton distributions at NLO; the dotted and dot-dashed lines correspond to the twist-4 and twist-6 terms, respectively.

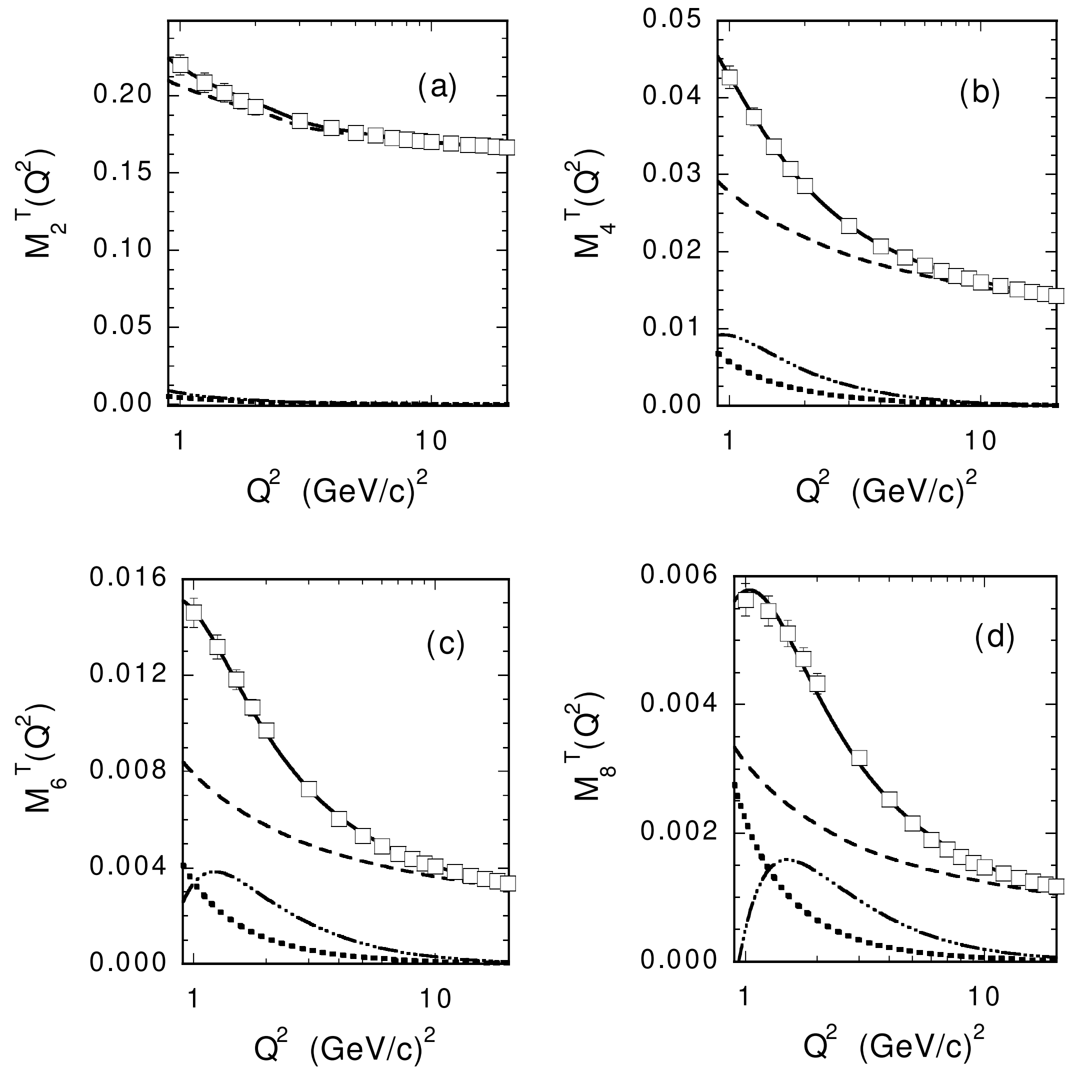

Figure 1.3: Twist analysis of the proton transverse moments $M_n^T(Q^2)$ for $n = 2, 4, 6$ and 8, including both phenomenological higher twists originating from multiparton correlations and the power corrections arising from the IR-renormalon model (see text). The values of the IR-renormalon parameters are fixed at $A_2^{IR} = -0.132$ GeV^2 and $A_4^{IR} = -0.009$ GeV^4, as resulting from the analysis of the longitudinal moments. The solid lines are the results fitted by the least-χ^2 procedure to the pseudo-data (open squares); the dashed lines are the twist-2 contribution, while the dotted and dot-dashed lines correspond to the IR-renormalon and multiparton correlation contribution respectively.

3. The lowest $n = 2$ transverse moment (related to the average x dependence of the F_2 structure function) is well reproduced by the NLO twist 2 calculation, the contribu-

tion of renormalon terms and higher twists being almost negligible in this moment.

4. For higher $n = 4, 6, 8$ moments, related to F_2 data at large x, the twist 4 and twist 6 contributions have opposite sign [7]. Moreover, the two corresponding renormalon terms have opposing sign. Therefore, the higher moments have compensating effects on the suture function F_2.

   The last two points illustrate in moments space the well known "local duality" of the transverse structure function and corresponding precocious scaling often observed in low Q^2 experiments [2, 3].

5. The analysis of deuteron pseudo data [7] shows a contribution of higher twists very similar to that observed in the proton. However the NLO twist two, extracted from the expansion 1.3 is systematically larger for $n > 2$ and all Q^2 than predictions of realistic parton models (like GRV) well fitted to proton data, while the inclusion of semi-empirical corrections for nuclear effects (dashed line) slightly increases the disagreement (Fig. 1.4). At large x values the inclusion of a possible enhancement of an empirical d quark parton distribution, as recently proposed [9], leads to a good agreement (full lines) with results [10] both for the proton and the deuteron (Fig. 1.4).

It should be noted that these conclusions have been reached using:

1. *interpolation* of existing DIS world data, i.e. numerical fit presently available in the literature, to cover the wide kinematic region required by the evaluation of $NM_n(Q^2)$ moments. This procedure considerably increases the errors on the evaluated moments since they must include the (given) fit uncertainty.

2. *extrapolation* of existing data, most at high beam energies, to the high x and low Q^2 region of great interest in this analysis. This procedure can introduce unexpected systematic errors particularly on the extraction of all power terms.

A direct evaluation of the $n > 2$ F_2 Nachtmann moments from data in the $0.5 < Q^2 < 5$ GeV^2 region using CLAS with the present and upgraded CEBAF beam will be a necessary complement to existing data analysis for a systematic understanding of high x parton physics in inclusive experiments.

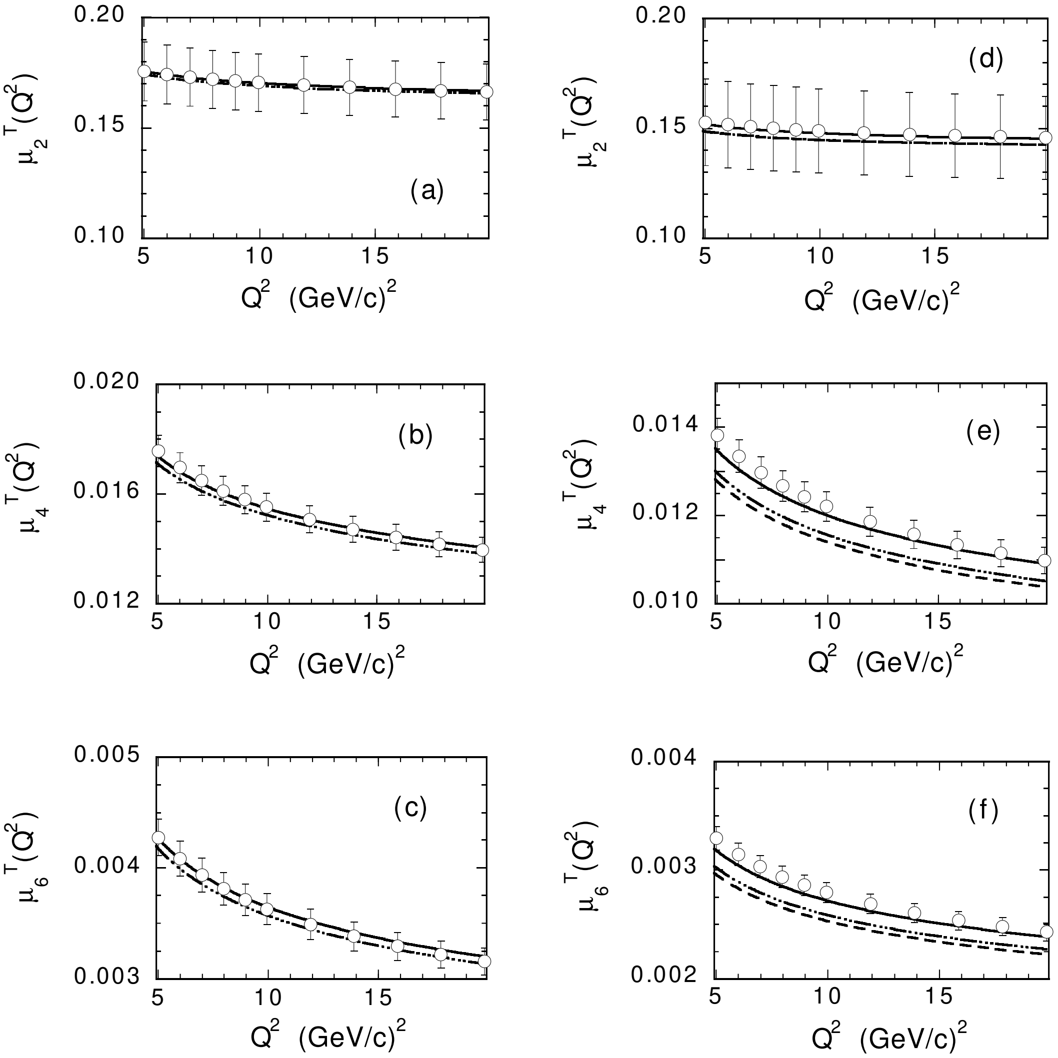

Figure 1.4: The leading-twist moments $\mu_n^T(Q^2)$ versus Q^2 for $n = 2, 4, 6$. Open dots: twist-2 extracted from our analysis of the proton and deuteron transverse pseudo-data, the errors represent the uncertainty of the fitting procedure corresponding to a one-unit increment of χ^2 per degree of freedom; dot-dashed lines: GRV prediction at NLO; dashed lines: the same as the dot-dashed lines, but including the empirical nuclear correction; solid lines: the same as dashed lines, but including the enhancement of the d-quark distribution at large x given explicitly by $\tilde{d}(x) = d(x) + 0.1x(1 + x)u(x)$.

1.3 Nuclei

For nuclei systematic investigations have been performed at high Q^2 values (EMC effect). However, in the $0.5 < Q^2 < 5$ GeV^2 interval, relevant for the extraction of higher twists, experimental data are still too sparse for quantitative evaluations.

Nevertheless, a preliminary analysis [10] for nuclei around mass 12, seems to provide some evidence that scaling in complex nuclei may be even more precocious than observed in the proton and deuteron:

1. In Fig. 1.5, Cornwell-Norton moments of the experimental F_2 structure function in $A = 12$ nuclei are presented, after mass corrections, in a $\log\log$ plot as a function of Q^2 in the $0.3 < Q^2 < 10$ GeV^2 range. The minimum momentum transfer where local duality provides an acceptable fit to the average inclusive inelastic cross section, should be related to the mass scale. The mass scale is defined as the minimum Q^2 where the moments of the structure functions begin to evolve according to twist two operators i.e. $M_n(Q^2) = A_n(Q^2)$ for $Q^2 > Q_0^2$ [7]. The Q^2 dependence of all moments should therefore exhibit a systematic change of slope at $Q^2 = Q_0^2 = \mu^2$ and then follow the perturbative QCD evolution (Eq. 1.1) which is linear in a $\log\log$ plot.

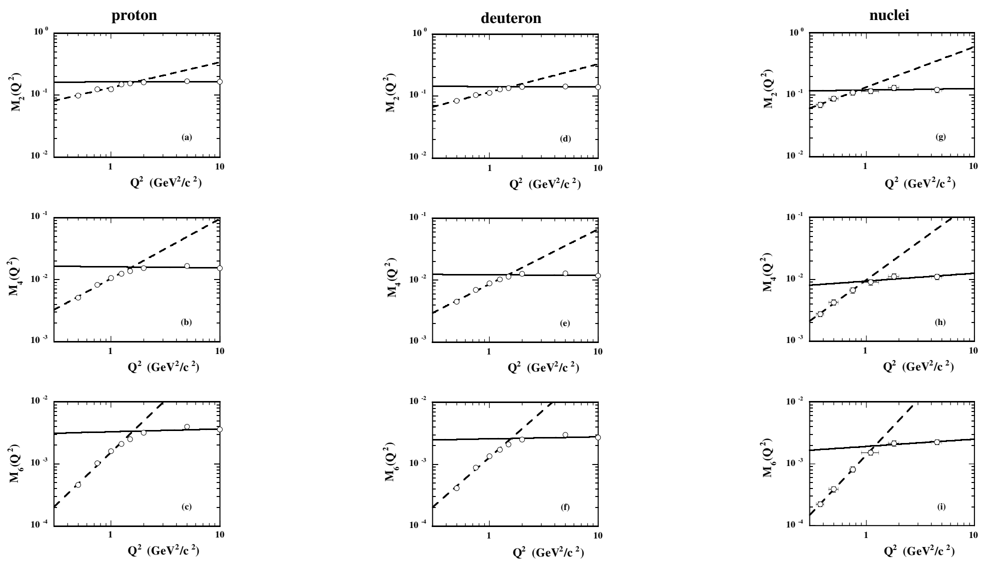

Figure 1.5: The moments $M_2(Q^2)$, $M_4(Q^2)$ and $M_6(Q^2)$, computed according to Eq. 1.1 for the proton (a,b,c), the deuteron (d,e,f) and nuclei with $A = 12$ (g,h,i) using the experimental data versus Q^2. The dashed and solid lines are linear fits to low- and high-Q^2 points respectively and are intended to show up the change of slope of the moments at $Q^2 \simeq Q_0^2$.

The expected systematic change of slope is clearly shown by all moments considered at the Q_0^2 values reported in the table:

Table 1.1: The minimum momentum transfer Q_0^2 where the moments are consistent with the leading twist behaviour for different target particles.

	$Q_0^2(M_2)$	$Q_0^2(M_4)$	$Q_0^2(M_6)$
Proton	1.6 ± 0.2	1.5 ± 0.1	1.6 ± 0.1
Deuteron	1.6 ± 0.1	1.5 ± 0.1	1.5 ± 0.1
Nuclei	0.8 ± 0.1	1.0 ± 0.2	1.2 ± 0.1

An interesting suggestion [7] is that, for existing data, *the onset of Bloom-Gilman local duality extends to a lower Q^2 values in complex nuclei with respect to the case of the proton and deuteron.*

2. If the relative deviation between experimental mass corrected moments $M_n(Q^2)$ and their pure twist 2 contribution $A_n(Q^2)$

$$\frac{\Delta M_n(Q^2)}{A_n(Q^2)} = \frac{M_n(Q^2) - A_N(Q^2)}{A_n(Q^2)} \tag{1.4}$$

is evaluated as a function of Q^2, the plot (Fig. 1.6) shows, inside the large errors affecting the available nuclear data, a rapid convergence toward twist 2 moments $A_n(Q^2)$ already at Q^2 values close to Q_0^2 in table 1.1.

These two points suggest the occurrence of the dominance of twist 2 operators for Q^2 values above the onset Q_0^2 reported in the table. This further precocity of local duality in nuclei, if confirmed, can be justified by different arguments. Two such arguments for the possible precocious local duality in nuclei are:

1. Partial quark deconfinement due to change of mass scale μ in nuclear matter. Moreover, quark deconfinement might also account for the faster decrease, with respect to the deuteron, of P_{33} and, perhaps, D_{13} resonance transition form factors observed [4] in light nuclei in a limited Q^2 range. Additionally, quark deconfinement, might explain the behaviour of the higher x part of EMC effect [11].

2. A quenching of higher twists in nuclear matter. This assumption, which is not currently supported by any theoretical predictions, remains an interesting speculation.

Whatever the speculation, the main conclusion is that: **experimental inclusive data at intermediate Q^2 are neither sufficient nor sufficiently precise** to afford any definite conclusions about possible nuclear matter effects in local duality. The previous discussion suggests that systematic measurements of the Q^2 evolution of: resonance

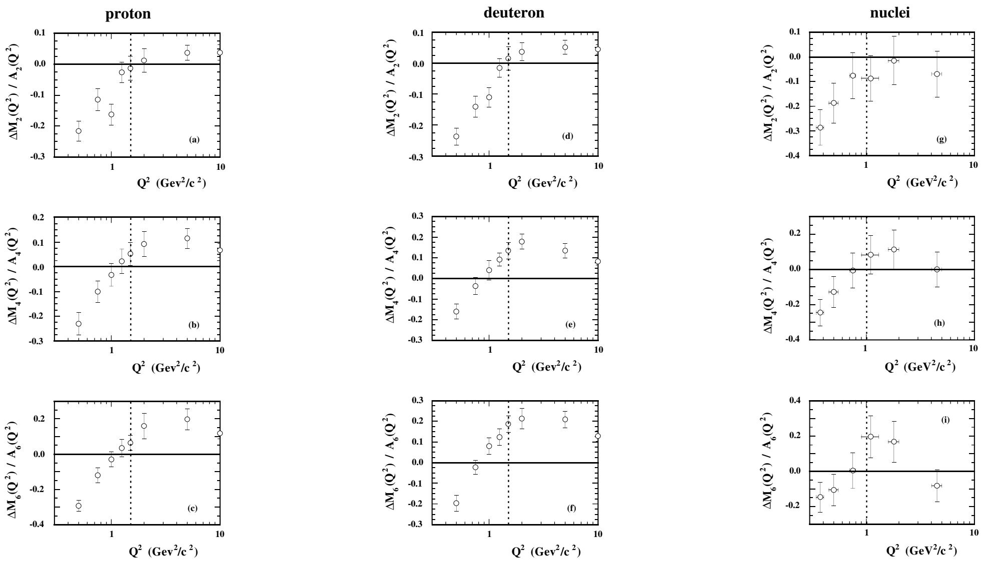

Figure 1.6: The relative deviation $\frac{\Delta M_n(Q^2)}{A_n(Q^2)}$ Eq. 1.4 of the experimental moments $M_n(Q^2)$, reported in Fig. 1.5, with respect to the leading twist moments $A_n(Q^2)$, calculated from Eq. 1.1 using the dual nucleon structure function properly folded with the nucleon motion in the nuclear medium. The vertical dotted lines are intended to show the approximate location of the static point $Q^2 \simeq \mu^2$, namely, $\mu_N^2 \simeq \mu_D^2 \simeq 1.5$ GeV^2 and $\mu_A^2 \simeq 1.0$ GeV^2.

transition form factors; moments $M_n(Q^2)$ $(n = 2, 4, 6, 8)$ of the $F_2(x, Q^2)$ structure function in the deep inelastic ($W > 2$ GeV) as well as resonance region **for different mass nuclei in $0.5 < Q^2 < 5$ GeV^2 range will be necessary to confirm and investigate any possible nuclear matter effects in duality region**.

Chapter 2

CLAS Data Analysis

The Thomas Jefferson National Accelerator Facility (TJNAF) can provide experimental information on the nucleon structure functions in the resonance region with unprecedented accuracy. The existing data, measured in Hall-C [12] do not allow a full integration of experimental values of the structure function $F_2(x, Q^2)$ over x at fixed Q^2. Approaches for an evaluation of the moments using different models of F_2, performed first in [7] with the SLAC function [13] and recently repeated [14] contain unknown systematic uncertainties generated by model dependence. Moreover, in case of nuclei, where few data exist and the Q^2 dependence of the structure function is completely unknown in the kinematic domain $0.1 < x < 1$, and $1 < Q^2 < 5$ GeV^2, the result of a such technique would be very uncertain. The CLAS data, which continuously covers the whole bidimensional kinematic region accessible at TJNAF, shown in Fig. 2.1, allows us to extract the moments based on experimental points over most of the integration range (see Fig. 2.2). While the expected data should have larger statistic and systematic uncertainties with respect to [12] and, therefore, do not give a competitive F_2 evaluation, the integration over x suppresses statistical errors leading to moments of good accuracy.

The proposed procedure of the experimental moments evaluation for proton and nuclear targets will be shortly described in next two sections.

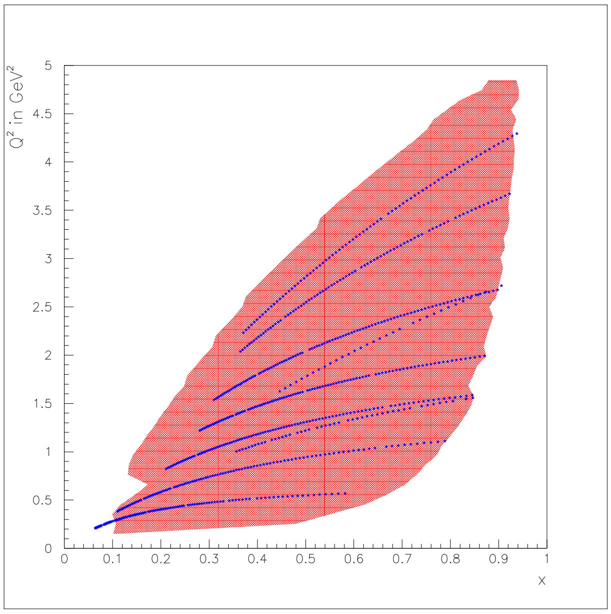

Figure 2.1: Kinematic range covered by the CLAS data: red area - the CLAS data; blue points - the Hall-C data.

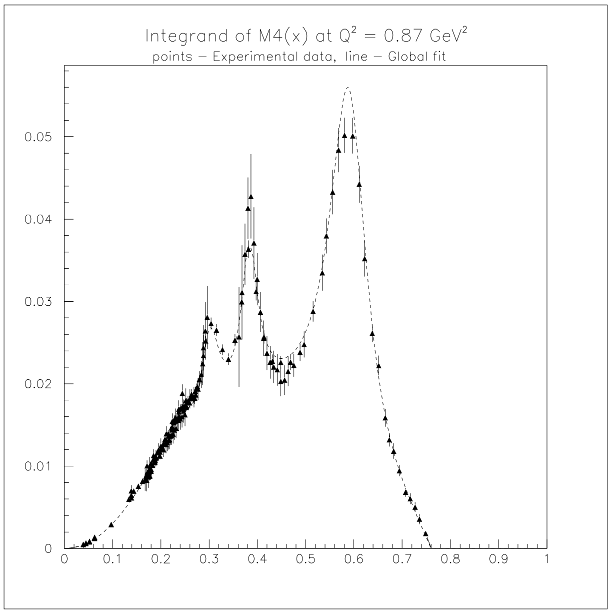

Figure 2.2: Integrand of M_4: points - all available $F_2(x, Q^2)$ data, including our preliminary results from the CLAS; dashed line - the global fit developed in [7].

2.1 The Proton

As explained in chapter 1, the final goal of this proposal is the evaluation of the Nachtmann moments $M_n^T(Q^2)$ of the structure function F_2:

$$M_n^T(Q^2) \equiv \int_0^1 dx \frac{\xi^{n+1}}{x^3} F_2(x,Q^2) \frac{3+3(n+1)r+n(n+2)r^2}{(n+2)(n+3)} \tag{2.1}$$

where $r \equiv \sqrt{1+4\frac{M^2x^2}{Q^2}}$ and $\xi \equiv \frac{2x}{1+r}$ is the Nachtmann variable.

The evaluation involves a computation of the integral over x from the structure function $F_2(x,Q^2)$ at fixed Q^2. The structure function $F_2(x,Q^2)$ will be extracted from the experimental inclusive inelastic cross section $\frac{d^2\sigma}{d\Omega dE'}$ using the fit of the ratio $R(x,Q^2) = \frac{\sigma_L}{\sigma_T}$ developed in [7], which is also reasonably valid for the resonance region:

$$F_2(x,Q^2) = \frac{1}{\sigma_{Mott}} \frac{d^2\sigma}{d\Omega dE'} \frac{\nu}{1+\frac{1-\epsilon}{\epsilon}\frac{1}{1+R}} \tag{2.2}$$

where the Mott cross section and the polarization parameter are defined as:

$$\begin{aligned} \epsilon &\equiv \left(1+2\frac{\nu^2+Q^2}{Q^2} tan^2\frac{\theta}{2}\right)^{-1} \\ \sigma_{Mott} &\equiv \frac{\alpha^2\cos^2\frac{\theta}{2}}{4E^2\sin^4\frac{\theta}{2}} \end{aligned}$$

The inclusive inelastic cross section will be evaluated from the number of well reconstructed events (requiring time based tracking and CC) $N(\theta,E')$, hitting a safe region of the detector, as follow:

$$\frac{d\sigma^2}{d\Omega dE'}_{rad}(\theta,E') = \frac{1}{\rho\frac{N_A}{M_A}LQ_{tot}} \frac{N_{H_2}(\theta,E')}{\Delta\phi\Delta E'\Delta\theta\sin\theta} F_{eff}(\theta,E')F_{pc}(\theta,E')F_{e^+e^-}(\theta,E') \tag{2.3}$$

where $\frac{d\sigma^2}{d\Omega dE'}_{rad}$ is the measured inclusive inelastic cross section; θ, E' are scattered electron angle and energy; N_A is Avogadro constant; M_A is the molar mass of the target substance; Q_{tot} is the total live-gated charge measured in FC; ρ is the density of the liquid H_2 in the target; L is the target length; $\Delta\theta$, $\Delta\phi$, $\Delta E'$ are corresponding bin sizes; $N_{H_2}(\theta,E')$ is number of events excluding the empty target contribution:

$$N_{H_2}(\theta,E') = N_{full}(\theta,E') - \frac{Q_{tot}}{Q_{tot_{empty}}} N_{empty}(\theta,E') \tag{2.4}$$

where N_{empty} and $Q_{tot_{empty}}$ are number of events and and charge, measured during empty target runs.

$F_{eff}(\theta, E')$ is the efficiency function; $F_{pc}(\theta, E')$ is the pion contamination correction function; $F_{e^+e^-}(\theta, E')$ is the pair production correction function.

The efficiency function $F_{eff}(\theta, E')$ will be extracted from a comparison of well known elastic cross section [15] with the measured one. This method allows an evaluation of the efficiency in the kinematic region shown in Fig. 2.3 using an interpolation procedure.

The trigger is not sufficient to remove all pion contamination (see Fig. 2.3), therefore an additional cut (shown by the black line in Fig. 2.3) will be applied in order to improve electron identification. The photoelectron spectra in the CC photomultiplier tubes will be studied in order to estimate a pion contamination:

$$F_{pc}(\theta, E') \equiv \frac{N_e(\theta, E')}{N_e(\theta, E') + N_\pi(\theta, E')} \tag{2.5}$$

where N_e and N_π are the number of electrons and pions in each kinematic bin respectively.

Since the positron data in the same kinematics are not available, the pair production background will be estimated according to the P. Bosted model [16], which appears to be in a good agreement with the EG1 experimental data. The pair production correction will be calculated as:

$$F_{e^+e^-}(\theta, E') = \frac{N_e(\theta, E')}{N_{e^+e^-}(\theta, E') + N_e(\theta, E')} \tag{2.6}$$

where N_e is number of inclusive electron events and $N_{e^+e^-}$ is number of electron-positron pairs created in the target.

The radiative correction can be applied following the "unfolding" procedure [17]; while internal bremsstrahlung can be estimated from fit [13].

Most important sources of systematic uncertainties, listed below, will be propagated to the moments:

1. The liquid target thickness stability during the data acquisition time.
2. Precision of the parameterization [15], used to obtain efficiency.
3. Radiative correction procedure contains an uncertainty of proton elastic form factors [15] as well as an uncertainty of the fit [13].
4. Precision of the model of $R(x, Q^2) = \frac{\sigma_L}{\sigma_T}$.

Preliminary analysis shows that overall systematic error of the proton structure function F_2 is lower than 10% (see Fig. 2.2); what leads to 1-3% uncertainties of the moments.

A preliminary analysis shows that the overall systematic error of the proton structure function F_2 is lower than 10% (see Fig. 2.2), this leads to an uncertainty of 1 to 3% for the moments.

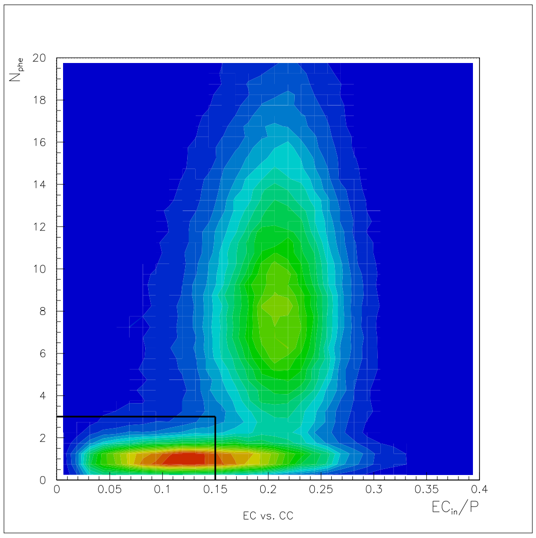

Figure 2.3: Energy deposited in inner calorimeter normalized to the particle momentum versus the number of photoelectrons detected in the CC ($E = 4$ GeV, $\theta \sim 30°$).

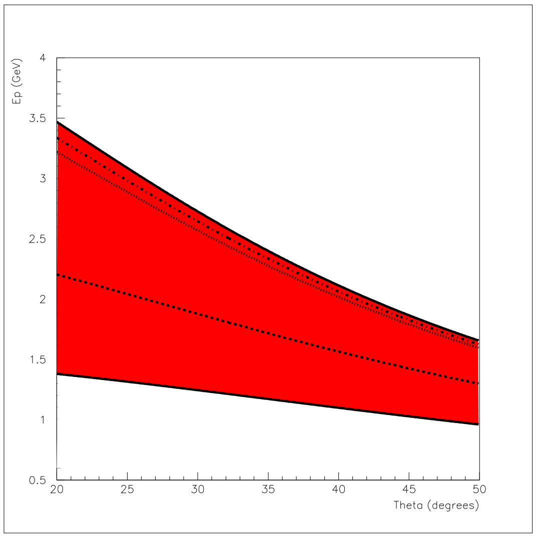

Figure 2.4: Kinematic area covered by the extracted efficiency: solid line - the elastic peak position at $E = 1.5$ GeV; dashed line - the elastic peak position at $E = 2.5$ GeV; dotted line - the elastic peak position at $E = 4.0$ GeV; dashed-dotted line (lower) - the elastic peak position at $E = 4.2$ GeV; dotted-dashed line (higher) - the elastic peak position at $E = 4.4$ GeV.

2.2 Nuclei

In the case of nuclei, only those parts different from the proton are discussed:

1. Since there is some amount of CH_2 data, the proton cross section can be extracted by a $CH_2 - {}^{12}C$ subtraction. The corresponding momentum correction and efficiency evaluation will be performed exactly following the method described above. Moreover, world data on the quasielastic [18] and inelastic cross section [19, 20, 21] could be used for these purposes if the amount of the CH_2 data appears insufficient.

2. Since the effect of the pair production contribution was negligible for the proton one could use parameterization [22] in order to obtain the correction function, even if this fit is not very accurate in our kinematic region. Moreover, contrary to the proton data, there is small amount of reverse field data for some beam energies, from which the correction could be estimated directly.

3. Radiative corrections require the nucleus elastic form factors [23, 24] and a model of the inelastic cross section to estimate internal bremsstrahlung [22].

4. Since $R_p = R_d = R_A$ [25, 26, 27, 28, 29] the proton fit of $R(x, Q^2) = \frac{\sigma_L}{\sigma_T}$ [7] will be used for the evaluation of the structure function F_2.

2.3 Future development

Preliminary analysis of the CLAS data performed on the proton demonstrated a very good agreement with previous world data measured at SLAC [12] and recent Hall-C data [13] as well.

The analysis pointed out a list of experimental conditions responsible for important corrections and accurate data normalization:

1. Availability of many data sets taken with different beam energies, desirable each 0.5 GeV, at fixed magnetic field setting could provide a very precise efficiency knowledge. Furthermore, these data could provide an evaluation of the ratio $R(x, Q^2) = \frac{\sigma_L(x,Q^2)}{\sigma_T(x,Q^2)}$ by the Rosenbluth separation in a wide kinematic range. Knowledge of $R(x, Q^2)$ is important for a precise $F_2(x, Q^2)$ extraction.

2. In the case of nuclei, a normalization of data could be performed using a comparison of two data sets corresponding to scattering off ${}^{12}C$ and CH_2 targets. Therefore, in addition to first point, E2 experiment should provide a sufficient quantity of CH_2 data for each beam energy and torus field setting.

In the future we may be interested in participating in proposals that can be used to further study of the nucleon structure described above.

Bibliography

[1] R. Roberts "The structure of the proton", Cambridge U.P. (1993).

[2] E. Bloom and F. Gilman, Phys. Rev. D4, 2901 (1971).

[3] C. Carlson and M. Mukhopadhyay, Phys. Rev. D47, 1737 (1993).

[4] M. Anghinolfi *et al.*, Nucl. Phys. A602, 405 (1996).

[5] M. Beneke, CERN TH/98-233 (1998).

[6] A. De Rujula, H. Georgi and H. Politzer, Ann. Phys. 103, 315 (1977).

[7] G. Ricco *et al.*, Nucl. Phys. B555, 306 (1999).

[8] CCFR coll., Phys. Rev. Lett. 79, 1213 (1997).

[9] U.Yang and A. Bodek Phys. Rev. Lett. 82, 2467 (1999).

[10] G. Ricco *et al.*, Phys. Rev. C57, 356 (1998).

[11] R. Jaffe, Phys. Rev. Lett. 50, 228 (1983).

[12] I. Niculescu, Ph.D. thesis, Hampton University (1999).

[13] A. Bodek *et al.*, Phys. Rev. D20, 1471 (1979).

[14] C. S. Armstrong *et al.*, Phys. Rev. D63, 094008 (2001).

[15] P. E. Bosted *et al.*, Phys. Rev. C51, 409 (1995).

[16] P. Bosted private communication.

[17] L. W. Mo and Y. S. Tsai, Rev. Mod. Phys. 41, 205 (1969).

[18] S. V. Dementii *et al.*, Sov. J. Nucl. Phys. 11 N1, 10 (1970).

[19] D. Zeller, Thesis, Karlsruhe (1973); and DESY internal report F23-73/2.

[20] D. B. Day *et al.*, Phys. Rev. C48, 1849 (1993).

[21] J. Arrington, Thesis, California Institute of Technology (1998).

[22] J.W. Lightbody, Jr. and J.S. O'Connell, Comp. in Phys. (1988).

[23] C. W. de Jager *et al.*, Atom. Nucl. Data Tables 14, 479 (1974).

[24] I. Sick *et al.*, Nucl. Phys. A150, 631 (1970).

[25] L. H. Tao *et al.*, Z. Phys. C70, 387 (1996).

[26] P. Amaudruz *et al.*, Phys. Lett. B294, 120 (1992).

[27] M. Arneodo *et al.*, Nucl. Phys. B487, 3 (1997).

[28] M. Arneodo *et al.*, Nucl. Phys. B481, 23 (1996).

[29] S. R. Dasu, Thesis, University of Rochester (1988).